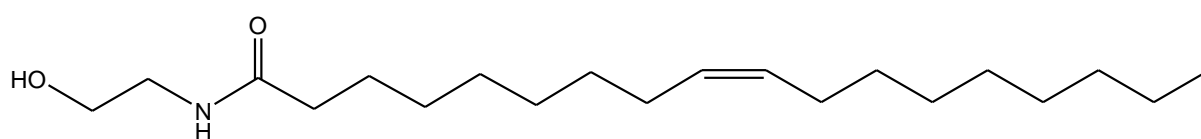


Supplemental Table 1: statistical significance levels of the variables displayed in figure 6 of the manuscript and representing the individual components of the biological clusters (an uppercase different letter in the same row indicates a significant difference, $P < 0.05$). *G, gene expression (arbitrary unit), B, biochemical determination, P, physiological assay.

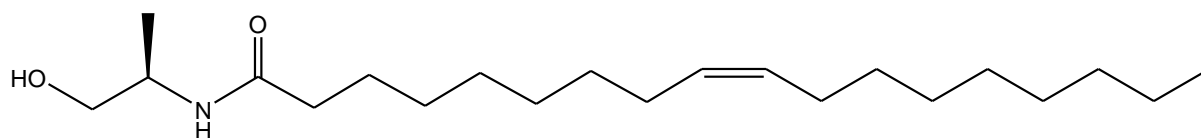
Variable name*	Control	OEA	KDS
G_CPT1intestine	0.8 ± 0.1^a	1.5 ± 0.2^b	1.3 ± 0.0^b
G_FAS liver	2.6 ± 0.2^a	4.3 ± 0.3^b	6.5 ± 0.6^c
G_SREBP1c liver	1.0 ± 0.1^a	1.4 ± 0.1^b	1.6 ± 0.1^c
G_SCD1 liver	5.5 ± 0.7^b	2.6 ± 0.2^a	2.9 ± 0.3^a
G_FAT/CD36 intestine	1.4 ± 0.2^b	2.3 ± 0.2^a	2.6 ± 0.2^a
G_FAT/CD36 AT ep	2.4 ± 0.4^b	1.3 ± 0.2^a	1.1 ± 0.1^a
G_FAT/CD36 liver			
G_PCSK9 liver	2.1 ± 0.2^a	3.0 ± 0.2^b	2.8 ± 0.1^b
G_FIAF AT ep	1.2 ± 0.1^b	0.9 ± 0.1^a	0.6 ± 0.0^a
G_FIAF AT per	0.4 ± 0.1^a	1.0 ± 0.1^b	1.2 ± 0.2^b
G_Ghrelin stomach	1.4 ± 0.2^a	2.9 ± 0.4^b	1.5 ± 0.2^a
G_GPR119 intestine	0.5 ± 0.0^a	1.0 ± 0.1^b	2.6 ± 0.4^c
G_CCK intestine	1.3 ± 0.2^a	2.0 ± 0.1^b	2.1 ± 0.2^b
G_Leptin AT ep	2.5 ± 0.6^a	8.4 ± 2.5^b	1.9 ± 0.5^b
G_CB1 AT per	1.7 ± 0.4^b	0.3 ± 0.1^a	0.6 ± 0.1^a
G_FAAH AT per	1.0 ± 0.1^a	1.5 ± 0.2^a	3.8 ± 0.5^b
G GLUT4 muscle	1.0 ± 0.1^a	3.1 ± 0.6^b	5.5 ± 0.2^c
G_G6P liver	1.7 ± 0.1^a	2.1 ± 0.2^{ab}	2.5 ± 0.2^b
P_Cumulated food intake (g)	103 ± 1.5^b	97 ± 0.9^a	98 ± 0.9^a
P_Respiratory quotient (AUC for post-prandial period)	522 ± 17	469 ± 15	474 ± 15
P_Spontaneous activity (post-prandial period, AU)	12 ± 1.8^a	17.4 ± 1.9^b	20 ± 2^b
P_Lipid oxidation ratio (post-prandial period)	0.5 ± 0.0^a	0.7 ± 0.1^b	0.7 ± 0.1^b
P_Glucose oxidation ratio (post-prandial period)	0.5 ± 0.0^b	0.3 ± 0.1^a	0.3 ± 0.1^a
B_FAAH intestinal activity (pmol/min*mg proteins)	2.0 ± 0.06^c	1.7 ± 0.2^b	1.0 ± 0.1^a
B_Plasma TG (mmol/L)	1.2 ± 0.1^b	0.9 ± 0.1^a	0.8 ± 0.1^a
B_HDL-cholesterol (mmol/L)	1.6 ± 0.0^b	1.4 ± 0.1^a	1.6 ± 0.0^{ab}
B_β-hydroxybutyrate (mg/mL)	0.07 ± 0.00^a	0.11 ± 0.01^b	0.11 ± 0.01^b

B_Liver FFA (mg/g)	0.4 ± 0.0^a	0.7 ± 0.1^b	0.4 ± 0.0^a
B_Liver glycerol (mmol/g)	2.7 ± 0.4^a	6.6 ± 0.7^b	5.2 ± 0.6^b
B_Plasma adiponectine (mg/mL)	4.1 ± 0.2^b	2.2 ± 0.4^a	4.1 ± 0.3^b
B-TG liver (mg/g liver)	261 ± 29^a	373 ± 47^b	264 ± 26^a

Figure 1.



Oleylethanolamide (OEA)



(Z)-(R)-9-Octadecenamide, N-(2-hydroxyethyl, 1-methyl (KDS-5104)

Supplementary methods

Indirect calorimetry. Between the third and the fourth week of treatment, each mouse was kept for 24h in an indirect calorimetric cage (Bioseb, Chaville, France). The calorimetric appliance was composed of a gas analyzer (to measure O₂ consumption and CO₂ production as VO₂ and VCO₂) and an activity recorder (locomotion and rearing). The calorimetric room of the animal facility was dedicated only to the current experiment with stable environment (23°C). Two cages were connected to each gas analyzer, but each cage had specific inlets and outlets. The inlet flow was steady throughout the experiment at 5cm³/min. The gases were analyzed continuously following the sequence of 3 min from cage 1, then 3 min from cage 2, then 3 min from room air and thus the volume (ml/min) of O₂ consumed (VO₂) and CO₂ produced (VCO₂) were measured for each mouse. Energy expenditure (EE) was calculated as following ($EE = (16.3 * VO_2 + 4.57 * VCO_2) / 60$ (watt)). Lipid (LOX) and carbohydrate (GOX) oxidation were calculated according to the following equations: $LOX = (1.69 * VO_2 - 1.69 * VCO_2) * (9.46 * 4.186 / 60)$ (watt) and $GOX = (4.57 * VCO_2 - 3.23 * VO_2) * (3.74 * 4.186 / 60)$ (watt) (1). The total activity was evaluated by summing locomotion and rearing, and was normalized to the control average.

A second group of 24 mice was used to determine fat absorption. Similar to the previous groups, male C57bl6j mice were purchased at 8 weeks of age from Janvier Elevage (Le Genest-St-Isle, France), individually housed and fed *ad libitum* on a high fat diet and water for 2 weeks. Subsequently, the mice were randomly divided into 3 groups of 8 after blocking for body weight. These mice were fed the same high fat diet but with either 0.0, 0.1 g or 1.0 g of OEA per kg body weight, by addition to the diet, for 5 weeks. During the fourth week of feeding, the mice were kept for 5 days in metabolic cages to collect urine and faeces for evaluation of fat absorption.

Lipid analysis on liver. Total liver lipids were extracted using a mix of chloroform/methanol according to the method described by Folch *et al.* (2) and solubilized in isopropanol. Triglycerides (TG) concentration was determined using an enzymatic kit (Triglycerides GPO-PAP, Roche/Hitachi, Basel, Switzerland) and measuring absorbance at 492nm. Free fatty acids concentration in plasma was evaluated using an enzymatic kit from Wako/Oxoid (Fatty acids Wako Nefa c, Oxoid, Dardilly, France). Glycerol concentration in liver extract was measured using the first step of a TG titration kit (Free Glycerol Reagent, Sigma-aldrich, Saint-Louis, USA).

Analysis of plasma samples. Triglycerides (TG), glucose, total cholesterol and HDL cholesterol were directly measured on plasma samples collected during the sacrifice using a Beckman Coulter Systems SYNCHRON LX 20 (Beckman Coulter, Fullerton, USA). Free fatty acids concentration in plasma was evaluated using an enzymatic kit from Wako/Oxoid (Fatty acids Wako Nefa c, Oxoid, Dardilly, France). Glycerol concentration in plasma was evaluated using the first step of a TG titration kit (Free Glycerol Reagent, Sigma-aldrich, Saint-Louis, USA). 3-hydroxybutyrate concentration was measured using a colorimetric test according to the manufacturer's procedure (R-Biopharm AG, Darmstadt, Germany).

Faecal lipids determination. Feces were acidified using chloridric acid, then total fecal lipids were extracted using the method described by Folch *et al.* (2) using a mix of chloroform and methanol. Total lipids were weighted and results were normalized to fecal weight. Fat absorption was assessed using the following formula: Fat Absorption (%intake) = $100 * ((\text{Fat intake, g/d} - \text{faecal fat excretion, g/d}) / \text{fat intake, g/d})$.

RNA extraction and gene expression study. Total RNA from various tissue were extracted with TRIzol reagent (Invitrogen, Carlsbad, USA) according to the manufacturer's instruction. The RNA concentration was determined per nanodrop from the absorbance at 260 nm. Retro-transcription PCRs to synthesize cDNA were performed using an Applied

Biosystem Thermal Cycler 2720 and Superscript II (Invitrogen, Carlsbad, USA) according to the manufacturer's protocol. Real-time quantitative PCR (RT-qPCR) were performed on cDNA obtained as described before using a high throughput system (Biomek 3000, Beckman & Coulter, Fullerton, USA) and a Lightcycler 480 (Roche/Hitachi, Basel, Switzerland) with SYBR Green Master mix + kit (Eurogentec, Philadelphia, USA). Values are expressed as ratio of RNA levels relative to one control mice (diets with 0mg of OEA/kgBW) using $\Delta\Delta(Ct)$ (3).

In-vitro study of pancreatic lipase activity. Porcine lipase (AppliChem, Darmstadt, Germany) was diluted in 5 mM CaCl_2 to obtain a final activity of 300 U/L. Rosemary extract was diluted in DMSO to serve as the inhibitor. The enzyme and inhibitor were mixed in a 96 wells-plate and pre-incubated at 30°C for 5 min. The lipid substrate, containing 300 or 600 μM of OEA, was added to the well prior to an incubation of 20 min at 37°C. Optical density at 412 nm was determined at 10 minutes and 20 minutes. Activity was measured by QuantichromTM Lipase Assay Kit (BioAssay Systems, CA, USA) according to the manufacturer's instructions.

Intestinal FAAH activity. Reactions were conducted at 37°C for 10 minutes in 200 μL of Tris.HCl (50 mM, pH 8.0) containing fatty acid-free bovine serum albumin (0.1%), tissue homogenate (1 μg of protein) and [³H]-anandamide (1.5 nM; [³H]-AEA 40,000 dpm, American Radiolabeled Chemicals). Reactions were stopped by rapid addition of 400 μL ice-cold CHCl_3 -MeOH (1:1, v/v) and vigorous mixing. After centrifugation, radioactivity was counted by liquid scintillation in the aqueous layer. The results are expressed as pmol/min*mg of proteins and are the mean \pm SEM of three experiments performed in duplicate (supplemental online Table).

FAAH inhibition

FAAH inhibition was assessed by measuring the hydrolysis of a radiolabeled substrate ($[^3\text{H}]$ -AEA, 60 Ci/mmol) as previously reported (4). Briefly, recombinant FAAH (0.8 μg of protein/tube) in Tris-HCl (165 mL, 100 mM, pH 7.4, 0.1% w/v fatty acid-free BSA [final]) was added to glass tubes that contained either 10 μL of drug in DMSO or DMSO alone (control). Hydrolysis was initiated by adding a solution of $[^3\text{H}]$ -AEA in Tris-HCl (25 μL , 50000 dpm; 2 μM final concentration). Tubes were incubated in a shaking water bath at 37°C for 10 min. Tubes containing buffer only (blank) were used as controls for chemical hydrolysis (blank) and this value was systematically subtracted. Reactions were stopped by adding ice-cold MeOH-CHCl₃ (1:1, 400 μL), and the radiolabeled ethanolamine was extracted by mixing and subsequent centrifugation at 1700*g (5 min). The upper layer (200 μL) was recovered and the radioactivity was measured by liquid scintillation. The data are the mean \pm SEM of three experiments performed in duplicate.

OEA and KDS-5104 hydrolysis

Mouse brain and liver were homogenized in Tris.HCl (100mM, pH = 7.4) and subsequently centrifuged at 800*g for 15 min. The supernatant was discarded and the pellet resuspended in Tris buffer and centrifuged again (800*g, 15 min). The same operation was repeated once more, and the resulting final pellet resuspended in Tris buffer and assayed for protein content. Brain or liver homogenate (20mg of proteins/tubes) were added to glass tubes containing OEA or KDS (10 μM final) or DMSO (10 μL) and 190 μL of Tris.HCl buffer (100mM, pH = 7.4, 0.1% w/v fatty acid-free BSA) and incubated for 0h or 2h at 37°C. Reactions were stopped by rapidly adding 400 μL of an ice-cold mixture of MeOH-CHCl₃ (1:1). The resulting 1:2:2 buffer – MeOH – CHCl₃ mixtures were thoroughly mixed before adding 5 μL of d-OEA (40 μM) as internal standard. After vortexing, the tubes were centrifuged (800*g, 5 min) and 175 μL of the organic phase (containing the intact OEA and KDS-5104) recovered. The solution was evaporated under N₂ stream and the residue recovered in 20 μL of MeOH-CHCl₃

(1:1). The resulting fraction was analyzed by HPLC-MS using an LTQ Orbitrap mass spectrometer (ThermoFisher Scientific) coupled to an Accela HPLC system (ThermoFisher Scientific). Analyte separation was achieved using a C-18 Supelguard pre-column and a Supelcosil LC-18 column (3 μ m, 4x150mm) (Sigma-Aldrich). Mobile phases A and B were composed of MeOH-H₂O-acetic acid 75:25:0.1 (v/v/v) and MeOH acetic acid 100:0.1 (v/v), respectively. The gradient (0.5 ml/min) was designed as follows: transition from 100% A to 100% B linearly over 15 min, followed by 10 min at 100% B and subsequent re-equilibration at 100% A. We performed MS analysis in the positive mode with an APCI ionization source. The capillary and APCI vaporizer temperatures were set at 250°C and 400°C, respectively. Both OEA and KDS-5104 levels were normalized to the levels of the internal standard d-OEA.

Statistical analysis

Multivariate

We used a multivariate statistical approach to obtain an integrated view of the biological impact of the treatments. The objective was to find among selected biological processes (manuscript Table 1) those mostly affected by both OEA and KDS administration and also associated to the reduction of body fat gain (see detailed description below). This included computation of the genes expression with the biochemical and physiological data that belong to the same string of biological events across various system biology levels and grouped as biological functions (manuscript Table 1), such as lipid transport, energy expenditure, energy intake, endocannabinoid signalling, lipogenesis, and glucose metabolism. Such a statistical approach (5) allows a semi-quantitation of the activity of each biological function under our nutritional challenge.

The statistical flowchart is presented in manuscript Figure 1 and explained in the material and method section.

Statistical model validations are reported in the following supplemental Table 2.

Supplemental Table 2. Statistics for discriminating the control, OEA, and KDS treated mice using each of the biological module variables, and to predict adipose fat gain (PLS1 model).

Biological module	Model fitting ¹ (PLS-DA or PLS* model with treatment as Y variable)		Intercept after permutation for control, OEA, and KDS, respectively ²		<i>P</i> value after CV- ANOVA ³	% Classification and <i>P</i> value (fisher prob) ⁴		
	R2Y	Q2Y	R2Y	Q2Y		Ctrl	OEA	KDS
Energy expenditure (2 components, 16 variables)	0.558	0.364	0.286	-0,375	0.001883	100	90	90
			0,244	-0,39		2.5×10^{-10}		
			0,305	-0,2989				
Lipogenesis (2 components, 12 variables)	0.616	0.461	0.186	-0.274	0.000171	90	80	90
			0.212	-0.21		4.1×10^{-8}		
			0.174	-0.254				
Lipid transport (2 components, 17 variables)	0.687	0.522	0.22	-0.223	0.000034	90	100	100
			0.195	-0.262		9×10^{-12}		
			0,207	-0,230				
Glucose metabolism (2 components, 7 variables,)	0.673	0.577	0.134	-0,222	0.000011	100	90	90
			0,126	-0.262		1.4×10^{-10}		
			0.098	-0.237				
Energy intake (2 components, 8 variables)	0.601	0.504	0.16	-0.21	0.000095	70	90	100
			0.166	-0.216		1.2×10^{-8}		
			0.125	-0.261				
Endocannabinoid signalling (2 components, 12 variables)	0.732	0.628	0.234	-0.389	0.000118	100	100	100
			0.249	-0.39		2.9×10^{-13}		
			0.232	-0.436				
All variables together	0.884	0.803	0.38	-0.249	$2,72 \times 10^{-13}$	100	100	100

(2 components, 69 variables)			0.417	-0.265		2.9×10^{-13}
			0.39	0.291		
All variables to adipose fat gain (PLS1, 1 component, 69 variables)*	0.56	0.34	0.50	-0.13	0.0087	-

¹R²Y, fraction of the group variance modeled by all components, Q²Y, predictable fraction of the group variance modeled by all components after cross validation (R²Y should be > 0.5 and Q²Y > ½ x R²Y).

²compare the goodness of fit (R² and Q²) of the original model with the goodness of fit of several models based on data where the order of the Y-observations (class assignment) has been randomly permuted, while the X-matrix (biological variables) has been kept intact. R²Y and mostly Q²Y must decrease when observations are permuted across classes; especially, Q²Y must have negative values with the intercept of the vertical axis.

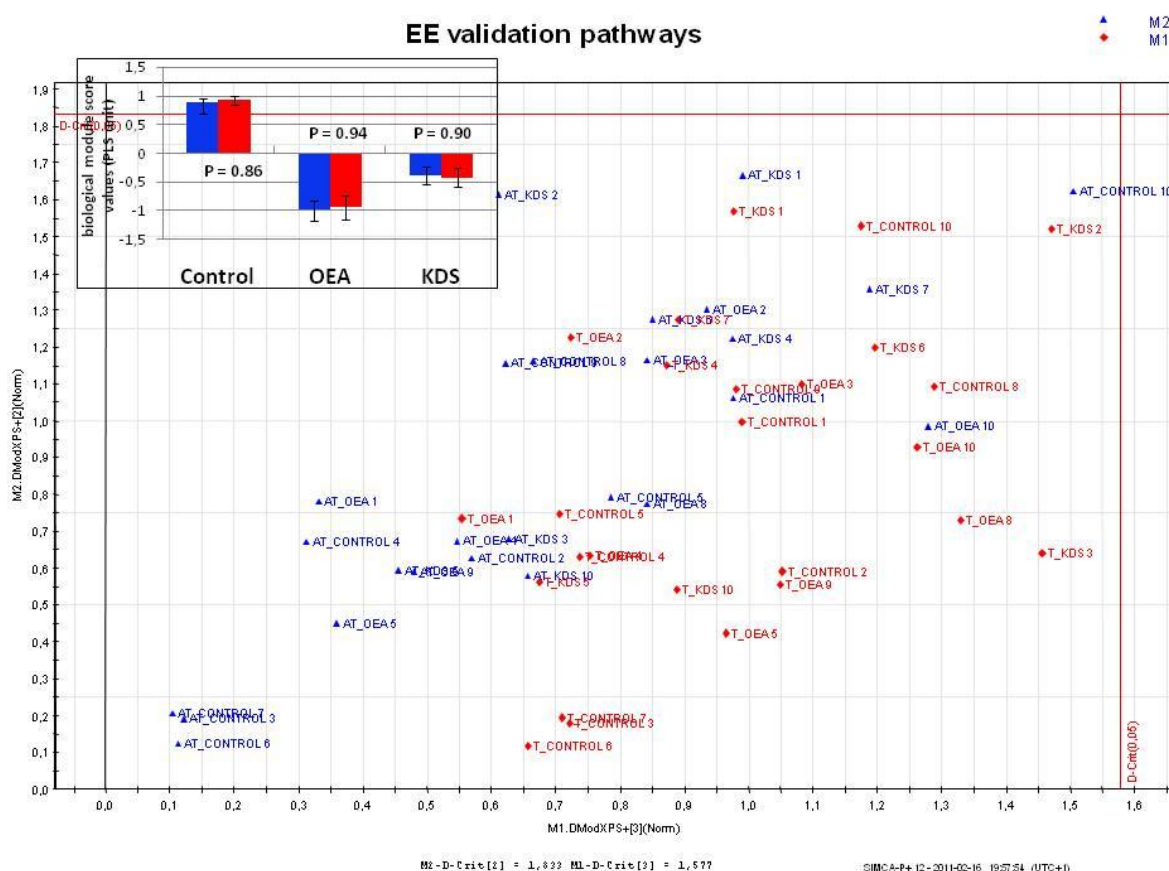
³*The significance of the PLS model can also be estimated through response permutation testing. The method first estimates a PLS model and its R²Y and Q²Y; then, with X fixed, the order of the elements in the Y-vector is randomly permuted a number of times, say 100–1000 times. Each time a new PLS model is fitted using X and the permuted Y, providing a reference distribution of R²Y and Q²Y for random data. These distributions are then used to appraise the statistical significance of the R²Y- and Q²Y-parameters of the original ‘unperturbed’ PLS model’; CV-ANOVA uses an F-test for the significance test (hypothesis test) of the null hypothesis of equal residuals of the two model (from Erickson, K. L., J. Trygg, and S. Wold. 2008. CV-ANOVA for significance testing of PLS and OPLS1 models. *J. Chemometrics* **22**: 594–600).*

⁴Correct classification rate obtained from the respective PLS-DA models and calculated from the misclassification function of the SIMCA software. The *P* value is indicated for each model.

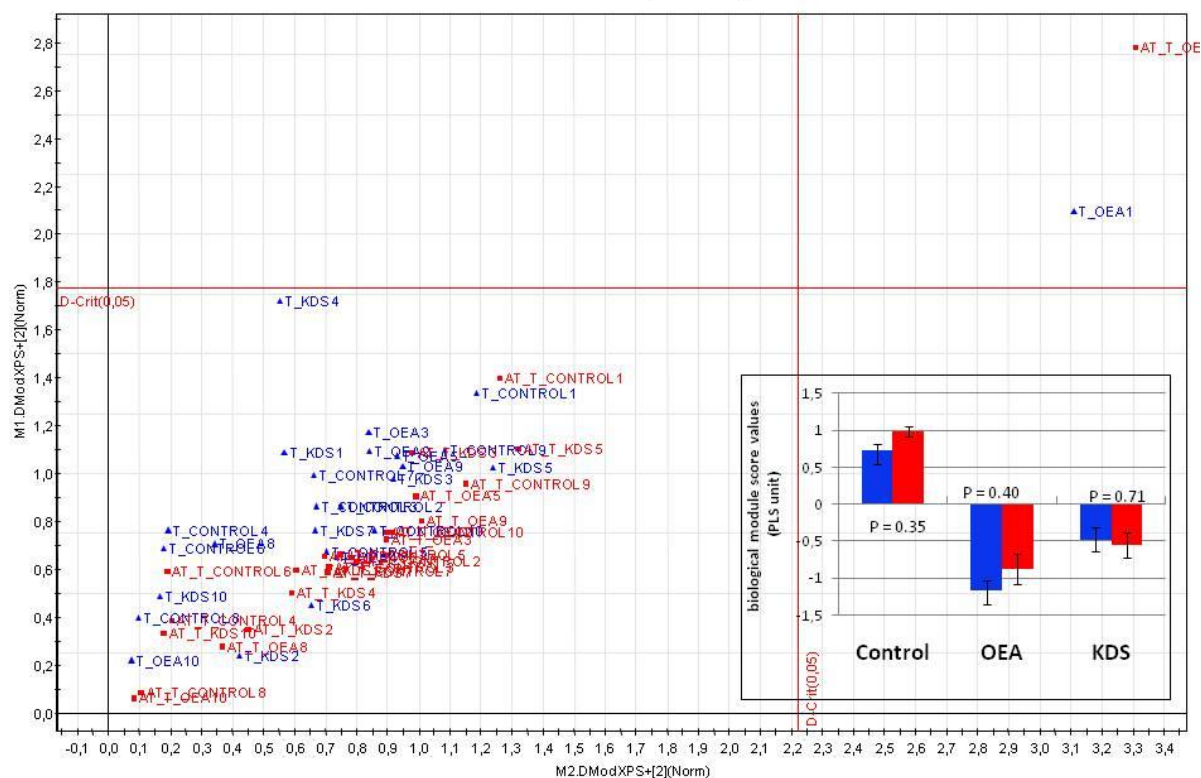
To compare the biological module responses obtained either with all the variables or only with the selected variables, we used Cooman’s plot of the NIPALS algorithm. The Cooman's plot describes the class boundaries for samples with the complete set of variables or after variables selection. The majority of the samples with variables selection lie within the tolerance of the original samples indicating that variables selection produced no overt biological module activity changes in our conditions.

In addition, we also compared for each module the scores obtained by hierarchical PLS before and after variables selection. In each situation the t-test performed indicated that no difference occurred before and after variables selection, thus corroborating the Cooman's plot findings.

Below are the figures displaying the Cooman's plot for each biological module (blue, before variables selection; red, after variables selection); the boundaries of class assignment with the critical distances are indicated by red lines; as an additional confirmation, the insert shows the group samples scores values calculated by hierarchical PLS with the *P*-value before and after variables selection (t-test, same color code than for the Cooman's plot). EE, energy expenditure module; EI, energy intake module, ES, endocannabinoid signaling module, GM, glucose metabolism, module, LG, lipogenesis module; LT, lipid transport module. The shift of the scores values induced by variables selection is not significant, indicating that the selected variables are representative of the whole pathway response.

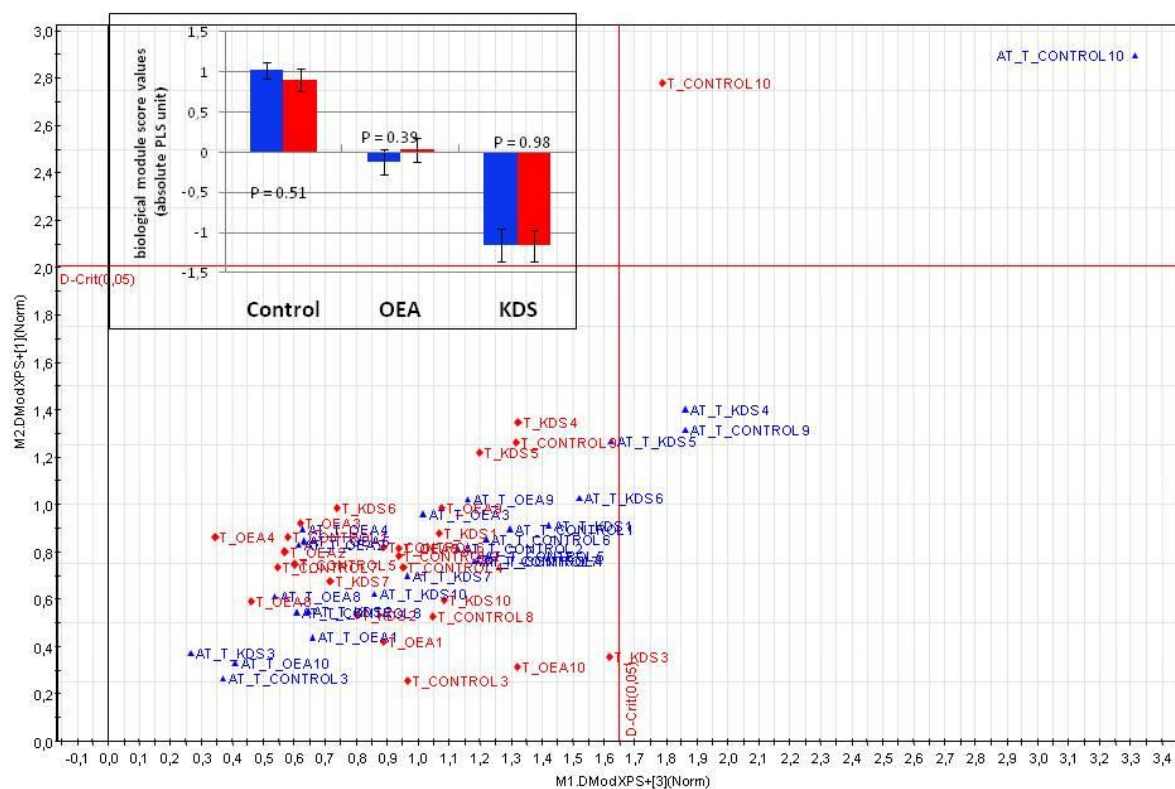


 M1
 M2



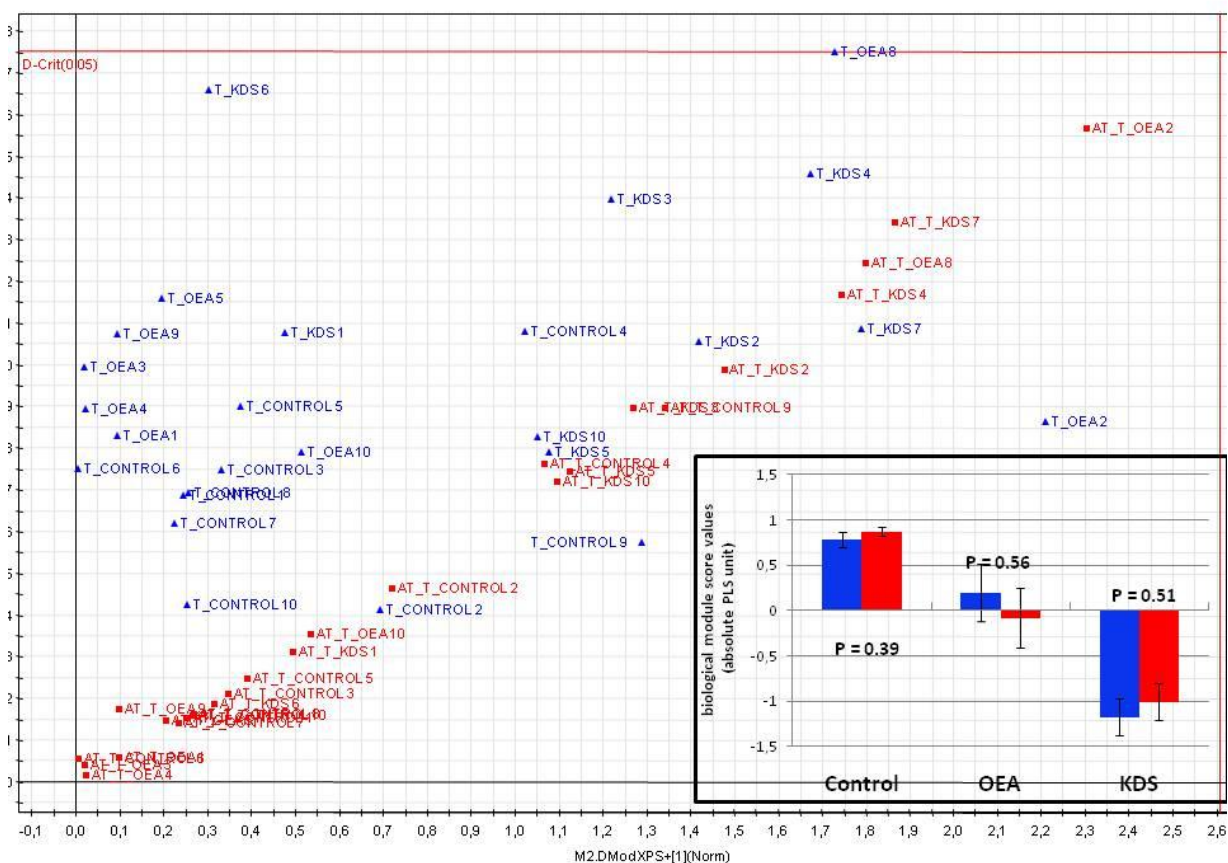
SIMCA-P+ 12-2011-02-17 10:19:45 (UTC+0)

M2
M1

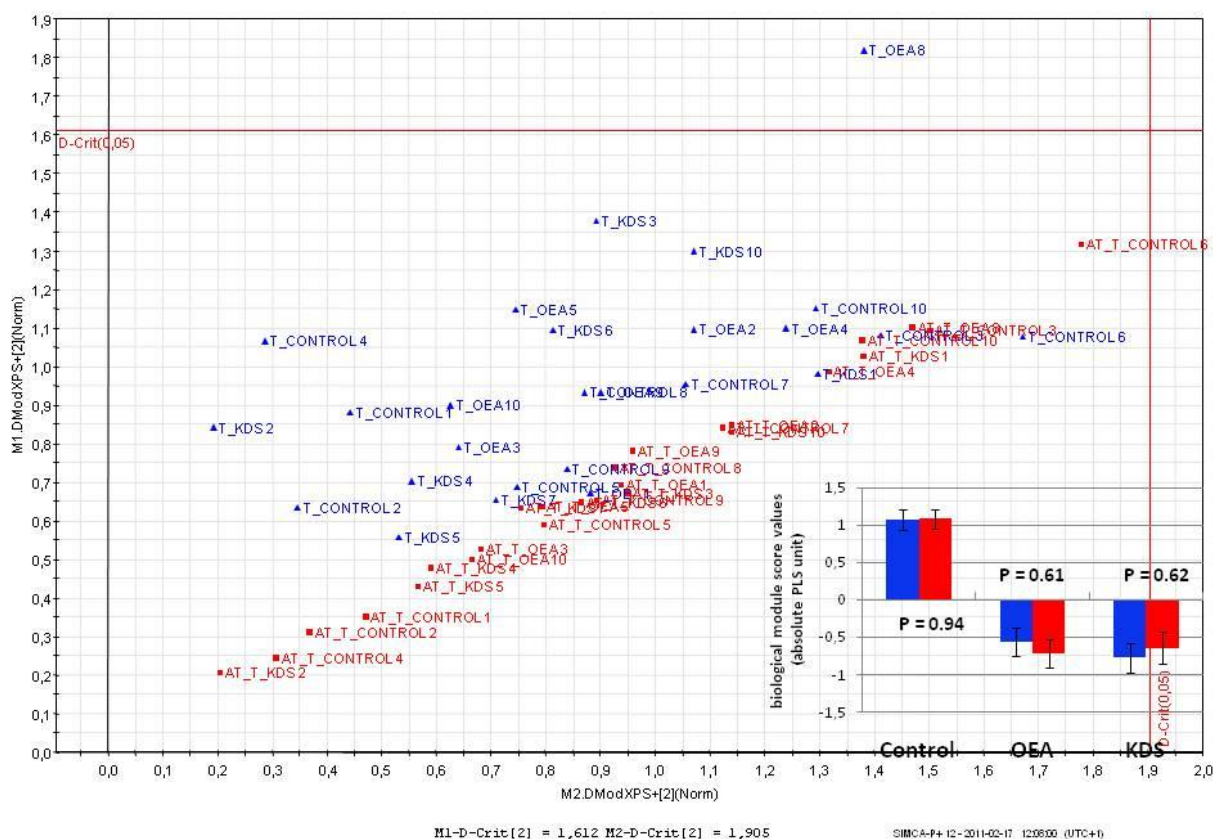


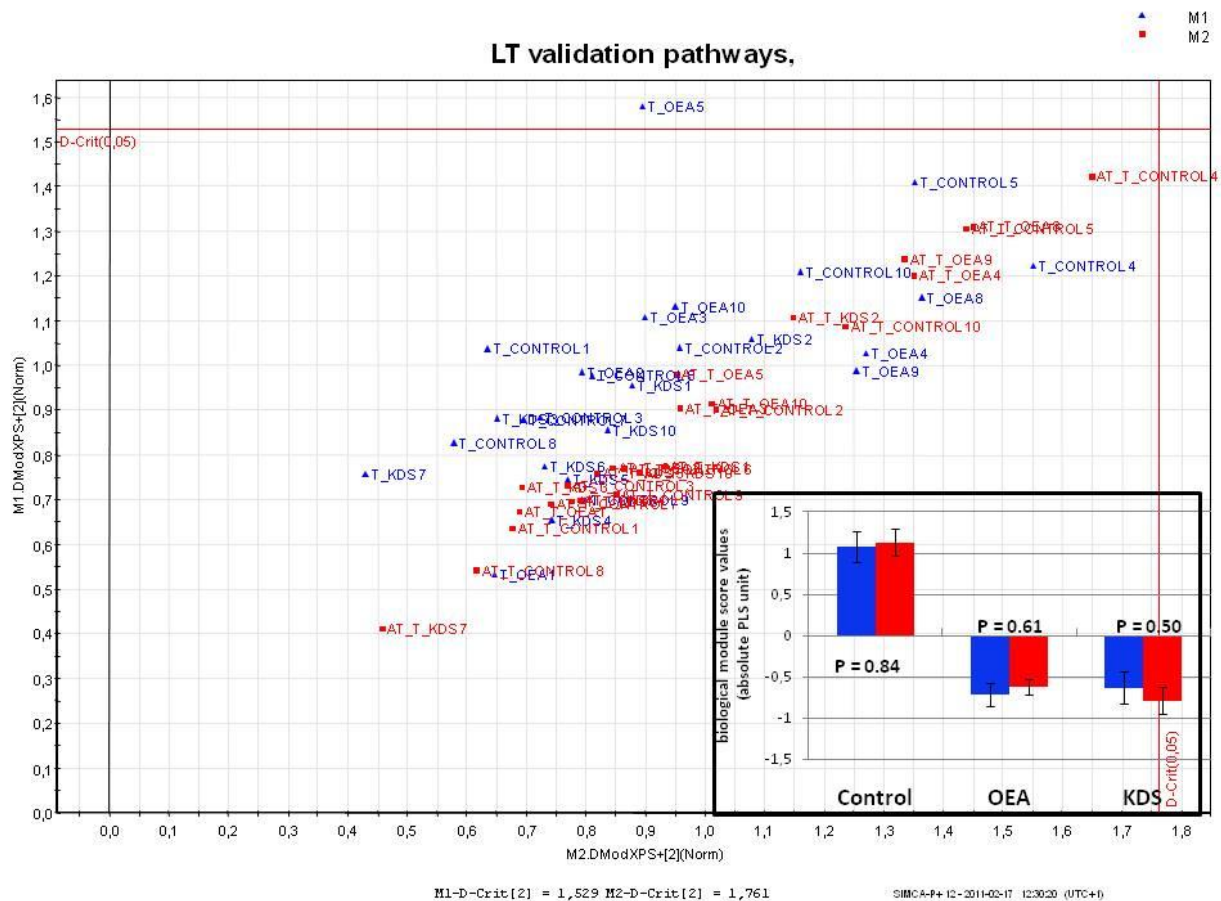
SIMCA-P+ 12-2011-02-17 10:43:30 (UTC+1)

GM validation pathways



LG validation pathways





Hence, to summarize, we first determined that each biological module was responsive to treatment (Table 2 above), and that the variables selected for both treatment responsiveness and adipose fat variations reflected well the biological module response to OEA and to its non-hydrolyzing analog prior to variables selection (Cooman's plot and *t*-test on latent variables).

1. Even, P. C., A. Mokhtarian, and A. Pele. 1994. Practical aspects of indirect calorimetry in laboratory animals. *Neurosci Biobehav Rev* **18**: 435-447.
2. Folch, J., M. Lees, and G. H. S. Stanley. 1957. A simple method for the isolation and purification of total lipids from animal tissues. *J. Biol. Chem.* **226**: 497-509.
3. Livak, K. J., and T. D. Schmittgen. 2001. Analysis of relative gene expression data using real-time quantitative PCR and the 2(-Delta Delta C(T)) Method. *Methods* **25**: 402-408.
4. Muccioli, G. G., C. Xu, E. Odah, E. Cudaback, J. A. Cisneros, D. M. Lambert, M. L. Lopez Rodriguez, S. Bajjalieh, and N. Stella. 2007. Identification of a novel endocannabinoid-hydrolyzing enzyme expressed by microglial cells. *J Neurosci* **27**: 2883-2889.
5. Wold, S., N. Kettaneh, and K. Tjessem. 1996. Hierarchical multiblock PLS and PC models for easier model interpretation and as an alternative to variable selection *Journal of Chemometrics* **10**: 463-482.